

# Thermally assisted magnetization reversal of a magnetic nanoparticle driven by a down-chirp microwave field pulse

M. T. Islam<sup>a,\*</sup>, M. A. J. Pikul<sup>a</sup>, X. S. Wang<sup>b</sup> and X. R. Wang<sup>c,d</sup>

<sup>a</sup>Physics Discipline, Khulna University, Khulna 9208, Bangladesh

<sup>b</sup>Center for Quantum Spintronics, Department of Physics, Norwegian University of Science and Technology, NO-7491 Trondheim, Norway

<sup>c</sup>Physics Department, Hong Kong University of Science and Technology, Clear Water Bay, Kowloon, Hong Kong

<sup>d</sup>HKUST Shenzhen Research Institute, Shenzhen 518057, People's Republic of China

## ARTICLE INFO

### Keywords:

Magnetization reversal  
Thermal effect  
sLLG equation  
Energy barrier  
Stability factor

## ABSTRACT

Fast magnetization reversal of a single-domain magnetic nanoparticle can be achieved by a linear down-chirp microwave field pulse (DCMWP) in zero temperature limit. Certain requirements for the microwave wave amplitude, chirp rate, and initial frequency have to be satisfied for the reversal. However, the generation of such DCMWP in practice is a challenging issue, and the finite temperature is ubiquitous in practice. Here, we study the effect of finite temperature on DCMWP-induced magnetization reversal based on the stochastic Landau-Lifshitz-Gilbert equation. It is found that the DCMWP with significantly smaller amplitude, chirp rates, and initial frequency induces fast and more energy efficient magnetization reversal. The critical temperature, which is defined as the maximal temperature at which fast and energy-efficient reversal is valid, increases with enlarging the system size and hence a wide operating temperature above room temperature is possible in reality. It is because the energy barrier/thermal stability increases with the volume of the system, but the effective magnetization decreases with temperature, which induces faster magnetization reversal. These findings may provide a way to realize low-cost and fast magnetization reversal with a wide operating temperature.

## 1. Introduction

Fast and energy-efficient magnetization reversal of magnetic nanoparticle draws much attention because of its application in non-volatile data storage device [1, 2, 3] and rapid information processing [4]. For practical realization, a wide range of operating temperature is required which can be obtained by employing the high-anisotropy materials which belong to higher energy barrier [5]. But the challenging issue is to find out the way to achieve the fastest magnetization reversal for high-anisotropy materials with a minimal energy. Purposely, in the early years, magnetization reversal was induced by a constant magnetic field [6, 7] which requires the larger reversal time [6] and it suffers from scalability and field localization issue for nano-device. The spin polarized electric current directly and/or indirectly becomes a potential candidate to induce magnetization reversal by spin transfer torque from itinerant electrons and/or spin orbit torque from inter-facial electrons [8, 9, 10, 11, 12, 13, 14, 15, 16, 17, 18, 19, 20, 21, 22].

However, in case of the STT-MRAM or SOT-MRAM based device fabrication, the requirement of a large current density is an obstacle since it generates Joule heat which limits the device durability and reliability [23, 24, 25, 26, 27, 28, 29]. Later on, people digress to utilize the microwave field of constant or time dependent frequency, either with or without a polarized electric current, to induce magnetization reversal [30, 31, 32, 33, 34, 35, 36, 37, 38].

But the requirement of the large field amplitude and the long reversal time are emerged as limitations to realized the

microwave (of constant or time dependent frequency) induced magnetization reversal device [39, 40, 41].

Recently, we proposed a model, refers to the study [42], in which a down-chirp microwave pulse (DCMWP) is capable of inducing subnanosecond magnetization reversal at temperature,  $T = 0$  K. But it requires the DCMWP, of a wide initial frequency range ( $\geq 21$  GHz), high chirp rate ( $\sim 67.2$  ns<sup>-2</sup>) and large critical amplitude (0.045 T), which is challenging to generate in practice and the model does not include thermal effect. However, there are several studies demonstrating the thermal effect assists magnetization reversal induced by magnetic field or electric current [43, 44, 45, 46, 47], which is because the magnetization of the sample decreases with temperature and hence the effective anisotropy ( $K_{\text{eff}} = \frac{M_s \times H_k}{2}$ ) or the energy barrier ( $E_b = K_{\text{eff}}V$ ) decreases, where  $V$  is the volume of the system. Consequently, the magnetization reversal at finite temperature  $T > 0$  becomes faster even with smaller magnetic field and current than that of at  $T = 0$ .

Therefore, this study motivates to investigate the finite thermal effect on magnetization reversal of single domain nano-particle induced by DCMWP focusing on how the thermal effect influences the magnetization reversal process and the parameters of DCMWP. Furthermore, it is investigated how the critical temperature of magnetization reversal is affected by the increase of volume of the system since the energy barrier,  $E_b \propto V$ .

Interestingly, it is found that the thermal effect assists the magnetization reversal induced by the DCMWP and significantly reduces the critical amplitude, chirp rates, and initial frequency. In addition, the critical temperature increases with enlarging the system size and hence a wide operating

\*Corresponding author: torikul@phy.ku.ac.bd

ORCID(S): 0000-0001-7511-2910 (M.T. Islam); 0000-0002-7500-1572 (M.A.J. Pikul); 0000-0002-8600-3258 (X.R. Wang)

temperature above room temperature is possible. Therefore, these findings may provide a way to realize low-cost and fast magnetization reversal with a wide operating temperature.

## 2. Analytical model and method

We consider a single-domain ferromagnetic nanoparticle (of different volumes) of perpendicular magnetization with finite temperature,  $T$  as shown in Fig. 1(a). The magnetization of nanoparticles is considered as a macrospin with magnetization direction  $\mathbf{m}$  along the  $z$  axis and magnitude  $M_s$ .

The magnetization dynamics, subject to the circularly polarized DCMWP and thermal field, is governed by the stochastic Landau Lifshitz Gilbert (sLLG) equation [48]

$$\frac{d\mathbf{m}}{dt} = -\gamma\mathbf{m} \times (\mathbf{H}_{\text{eff}} + \mathbf{h}_{\text{th}}) + \alpha\mathbf{m} \times \frac{\partial\mathbf{m}}{\partial t} \quad (1)$$

where  $\mathbf{m} = \mathbf{M}/M_s$  and  $M_s$  are the magnetization direction and the saturation magnetization.  $\alpha$  and  $\gamma$  are the Gilbert damping constant and gyromagnetic ratio respectively. The total effective field ( $\mathbf{H}_{\text{eff}}$ ) comes from the exchange interaction, the microwave magnetic field  $\mathbf{H}_{\text{mw}}$  and the anisotropy field  $\mathbf{H}_k = H_k m_z \hat{z}$ , i.e.,  $\mathbf{H}_{\text{eff}} = \frac{2A}{M_s} \sum_{\sigma} \frac{\partial\mathbf{m}}{\partial x_{\sigma}} + \mathbf{H}_{\text{mw}} + \mathbf{H}_k$ , where  $A$  is the exchange constant,  $x_{\sigma}$  ( $\sigma = 1, 2, 3$ ) denote Cartesian coordinates  $x, y, z$ , and  $\mathbf{h}_{\text{th}}$  is the stochastic thermal field.

The thermal field follows the Gaussian process characterized by following statistics

$$\begin{aligned} \langle h_{\text{th},ip}(t) \rangle &= 0, \\ \langle h_{\text{th},ip}(t) h_{\text{th},jq}(t + \Delta t) \rangle &= \frac{2k_B T_i \alpha_j}{\gamma M_s a^3} \delta_{ij} \delta_{pq} \delta(\Delta t), \end{aligned} \quad (2)$$

where  $i$  and  $j$  indicate the micromagnetic cells.  $p$  and  $q$  represent the Cartesian components of the thermal field.  $T_i$  and  $\alpha_j$  are respectively temperature and the Gilbert damping at cell size.  $k_B$  is the Boltzmann constant.

In the absence of external force and  $T$ , the magnetization of nanoparticle has two stable states  $\mathbf{m} = \mathbf{m}$  and  $\mathbf{m} = -\mathbf{m}$  because of two energy minima. To reverse the magnetization from one equilibrium state to the other, it is previously reported [42] that a circularly polarized DCMWP which takes the form  $\mathbf{H}_{\text{mw}} = H_{\text{mw}} [\cos \phi(t) \hat{x} + \sin \phi(t) \hat{y}]$ , where  $H_{\text{mw}}$  is the amplitude of the microwave field and  $\phi(t)$  is the phase, can induce fast reversal at zero temperature limit. The instantaneous frequency of DCMWP is  $f(t) \equiv \frac{1}{2\pi} \frac{d\phi}{dt}$  while the frequency linearly decreases (according to  $f(t) = f_0 - \eta t$ ) with the chirp rate  $\eta$  (with unit of  $\text{ns}^{-2}$ ) as shown in Fig. 1(b). The phase is  $\phi(t) = 2\pi(f_0 t - \frac{\eta}{2} t^2)$ , where  $f_0$  is the initial frequency at  $t = 0$ . The duration of the microwave pulse is  $\tau = \frac{2f_0}{\eta}$  so that the final frequency becomes  $-f_0$ .

Thus, subnanosecond magnetization reversal is achieved solely by the DCMWP [42] with the physical picture that it triggers stimulated microwave absorptions (emissions) by (from) the spin before (after) it crosses over the energy barrier at  $T = 0$ .

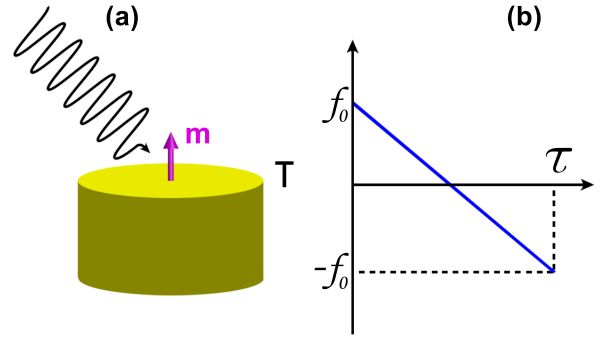


**Figure 1:** (a) Schematic diagram of the system in which  $\mathbf{m}$  and  $T$  represent unit vector of magnetization and temperature, respectively. A down-chirp microwave field is applied onto the single domain nanoparticle. (b) The frequency profile (sweeping from  $+f_0$  to  $-f_0$ ) of a down-chirp microwave.

However, for practical realization, a range of operating temperature around room temperature is required. The finite temperature is related to the thermal stability,  $\Delta = \frac{E_b}{k_B T}$ , where  $E_b$  is the energy barrier between parallel and anti-parallel states,  $T$  is the absolute temperature and  $k_B$  is the Boltzmann constant, which decreases with temperature for constant volume because of the diminution of energy barrier. In order to compensate for the loss of thermal stability/diminution of energy barrier at high temperature, the volume  $V$  of the system could be enlarged to increase the energy barrier ( $E_b = K_{\text{eff}} V$ ) as well as Curie temperature  $T_c$  while thermal energy ( $k_B T$ ) remains constant.

In the following investigation, the parameters are selected from the representative experiments on microwave-driven magnetization reversal as  $M_s = 10^6$  A/m,  $H_k = 0.75$  T,  $\gamma = 1.76 \times 10^{11}$  rad/(T · s),  $A = 13 \times 10^{-12}$  J/m, and  $\alpha = 0.01$ .

We use MuMax3 Package [49] to numerically solve stochastic LLG equation choosing adaptive Heun solver. To have efficiency as well as stability [50], we use the time step  $10^{-14}$  s and  $10^{-15}$  s with the cell size ( $2 \times 2 \times 2$ ) nm<sup>3</sup> and ( $0.5 \times 0.5 \times 0.5$ ) nm<sup>3</sup> respectively.

In this study, each numerical observation is obtained from the average of 12 random observations. We consider the switching time window 2 ns by which the magnetization reaches to  $m_z = -0.7$  (considering practical requirement).

## 3. Numerical Results

### 3.1. Temperature dependence of magnetization reversal and optimal chirp rate $\eta$

Since the thermal field induces a random fluctuation/disturbance to magnetic spin which might be useful also for fast and energy efficient the magnetization reversal induced

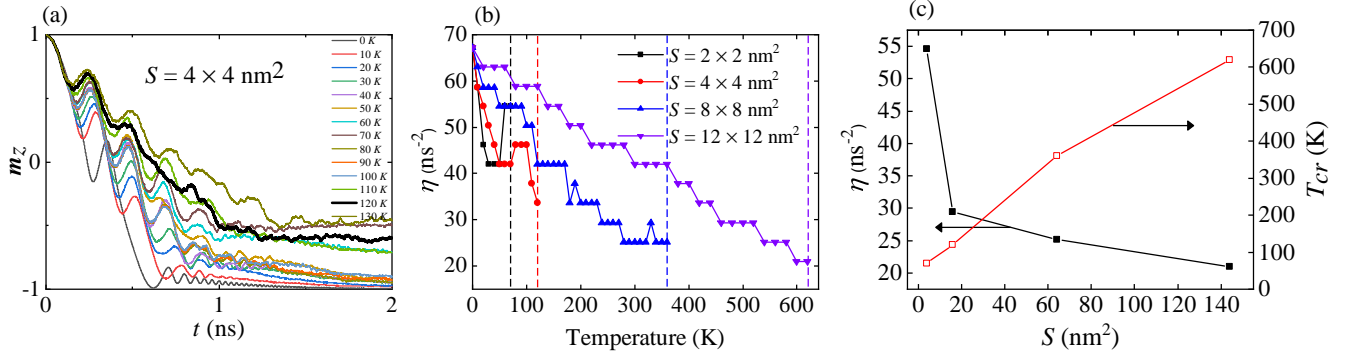


**Figure 2:** Model parameters of nanoparticle of  $M_s = 10^6 \text{ A/m}$ ,  $H_k = 0.75 \text{ T}$ ,  $\gamma = 1.76 \times 10^{11} \text{ rad}/(\text{T} \cdot \text{s})$ ,  $A = 13 \times 10^{-12} \text{ J/m}$ , and  $\alpha = 0.01$  (a) The time evolution of  $m_z$  of  $(4 \times 4) \text{ nm}^2$  driven by the DCMWP with  $f_0 = 21 \text{ GHz}$ ,  $H_{mw} = 0.045 \text{ T}$  and optimal chirp rates  $\eta$  for different  $T$ . (b) Optimal chirp rate  $\eta$  as a function of  $T$  for different cross-sectional areas  $S$ . (c) Estimated minimal  $\eta$  (solid squares) and critical temperature  $T_{cr}$  (open squares) as function  $S$ .

by the DCMWP. Purposely, at first, for the different thermal effect, we determine the optimal chirp rate  $\eta$  of the DCMWP (keeping the initial  $f_0 = 21 \text{ GHz}$  and amplitude  $H_{mw} = 0.045 \text{ T}$  constant) at which the reversal/switching time is minimal for the system of volume  $V = S \cdot t_{th} = (4 \times 4 \times 4) \text{ nm}^3$ , where  $S$  is the cross-sectional area and  $t_{th}$  is the thickness. In this study, the switching time  $t_s$  is defined as the time required to reach  $m_z = -0.7$ . The optimal DCMWP induced magnetization evolutions for the different thermal effects are shown in the Fig. 2 (a) for the system of  $S = (4 \times 4) \text{ nm}^2$ . It is observed that the magnetization dynamics at the beginning is not affected much as the magnetic particle stays at the bottom of the energy barrier. When the magnetic particle climbs up from the bottom of the energy barrier, the thermal effect started to affect the particle, and while crossing the energy barrier, the thermal effect becomes significant. With the increase of thermal effect, the microwave energy absorption (emission) by (from) the magnetization before (after) the barrier is reduced and hence magnetization reversal becomes hindered, consequently reversal time increases. After a certain temperature, the microwave energy absorption and/or emission is largely affected, and the magnetization does not switch or reach at  $m_z = -0.7$  which is referred as critical temperature  $T_{cr}$ . Bold (black) evolution in the Fig. 2 (a) shows the reversal at the critical temperature  $120 \text{ K}$  which is far below the room temperature. In order to increase the thermal stability, we investigate the magnetization reversal by enlarging the volume  $V = S \cdot t_{th}$  which increases the energy barrier (since  $E_b \propto S \cdot t_{th}$ , for constant anisotropy field) as well as Curie temperature  $T_c$  [43, 44, 45, 46, 47]. Purposely, the optimal chirp rates  $\eta$ 's are estimated as a function of temperature for the different cross-sectional areas  $S$ , i.e.,  $(2 \times 2) \text{ nm}^2$ ,  $(8 \times 8) \text{ nm}^2$ ,  $(8 \times 8) \text{ nm}^2$  and  $(12 \times 12) \text{ nm}^2$ . The magnetization reversal is found by the optimal DCMWP as a function of finite thermal effects with two interesting findings. One is that the chirp rate  $\eta$  decreases with rising temperature for each system size as

shown in the Fig. 2 (b). The decreasing rate of  $\eta$ , is faster for smaller  $S$  ( $2 \times 2) \text{ nm}^2$  whereas slower for larger  $S$  ( $12 \times 12) \text{ nm}^2$ . It is noted that  $\eta$  remains constant for a range of temperature which is useful in practice. Second finding is the critical temperature (indicated by dashed lines in Fig. 2 (b)) increases with  $S$  and goes beyond the room temperature. In the Fig. 2 (c), the minimal  $\eta$  and critical temperature  $T_{cr}$  are depicted as a function of cross-sectional area  $S$ . It is importantly noted that for  $(S = 12 \times 12) \text{ nm}^2$ , the minimal required  $\eta$  largely reduce to  $\sim 42 \text{ ns}^{-2}$  for the temperature range 300-360 K. This is an important finding from the practical point of view.

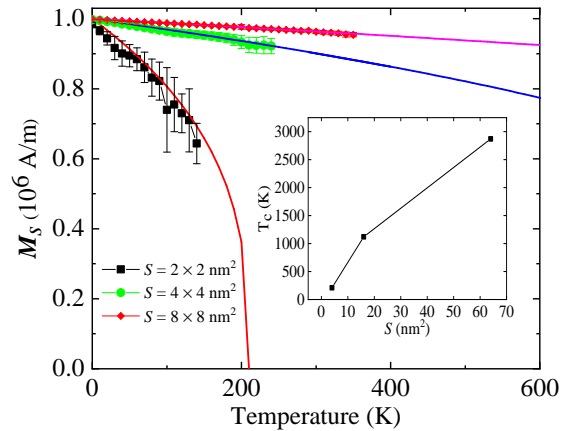


**Figure 3:**  $M_s$  is a function of  $T$  for different cross-sectional areas,  $S$ . Inset shows the Curie temperature,  $T_c$  as a function of cross-sectional area  $S$ .

In order to explain the decreasing (increasing) trend of the chirp rate  $\eta$  (the critical temperature  $T_{cr}$ ), we investigate the temperature dependence of saturation magnetization  $M_s$  as it is related to the effective anisotropy or energy barrier ( $K_{eff} = \frac{M_s \times H_k}{2}$ ). The  $M_s$  is numerically estimated as a function of  $T$  which are shown in the Fig. 3 for different  $S$ . It is

found that  $M_s$  decreases rapidly for smaller cross-sectional area  $S$  but with the increase of  $S$ ,  $M_s$  reduces slowly with  $T$ . This is happening because of the increment of the exchange energy with the  $S$  as it includes long range exchange interaction (super exchange interaction). The reduction of  $M_s$  with  $T$  follows the relation  $M_s(T) = M_0 \times (1 - \frac{T}{T_c})^{1/3}$  and hence by extrapolating the behaviour (line) as shown in the insets of the Fig. 3, we estimated the Curie temperature. The Curie temperature increases with cross-sectional area. However, as the length of  $M_s$  and hence the anisotropy are decreased, which reduces the height of the energy barrier. Therefore, the magnetization reversal becomes easier, and the requirement of optimal  $\eta$  decreases with temperature.

### 3.2. Temperature dependence of initial frequency $f_0$ and amplitude $H_{mw}$

Later on, we investigate whether there is any effect of temperature on initial frequency,  $f_0$  of the DCMWP which is almost to  $\frac{\gamma H_k}{2\pi}$ . Interestingly, we observe that  $f_0$  decreases with temperature,  $T$  for different cross-sectional area  $S$  as shown in the Fig. 4 (a). For smaller  $S$ , the decreasing rate is faster but for larger  $S$ , the decreasing rate is slower. These

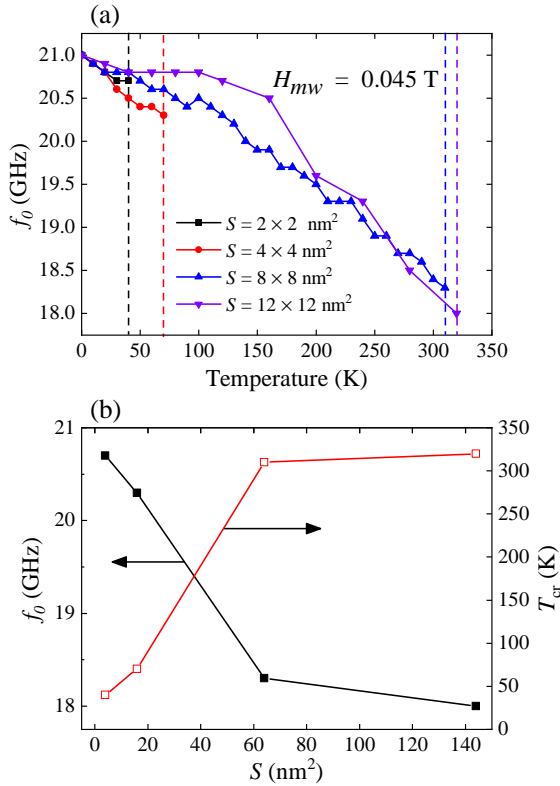


**Figure 4:** Temperature  $T$  dependence of (a)  $f_0$  (while  $H_{mw}$  and optimal  $\eta$  are constant) (b) optimal initial frequency  $f_0$  (solid squares) and critical temperature  $T_{cr}$  (open squares) as the function of  $S$ .

decrements have the similar reasoning: as the length of  $M_s$  decreases with temperature and hence effective anisotropy (is proportional to  $M_s^2$ ) decreases which lead to reduce the height of the energy barrier. The reduction rate of  $f_0$  and

$H_{mw}$  become slower for the larger system size. However, the critical temperature significantly increases with the enlarging of the system size, it is happened since the energy barrier is proportional to the volume of the system. Fig. 4 (b) shows the minimal required the initial frequency, as a function of cross-sectional area, which significantly reduces to 18 GHz for  $S = 12 \times 12 \text{ nm}^2$ . In addition, the critical temperature increases with the increase of  $S$  and estimated  $T_{cr} = 320 \text{ K}$  for  $S = 12 \times 12 \text{ nm}^2$ . Therefore, it is expected that initial frequency (critical temperature) could be decreased (increased) further for the larger nano-particle size.

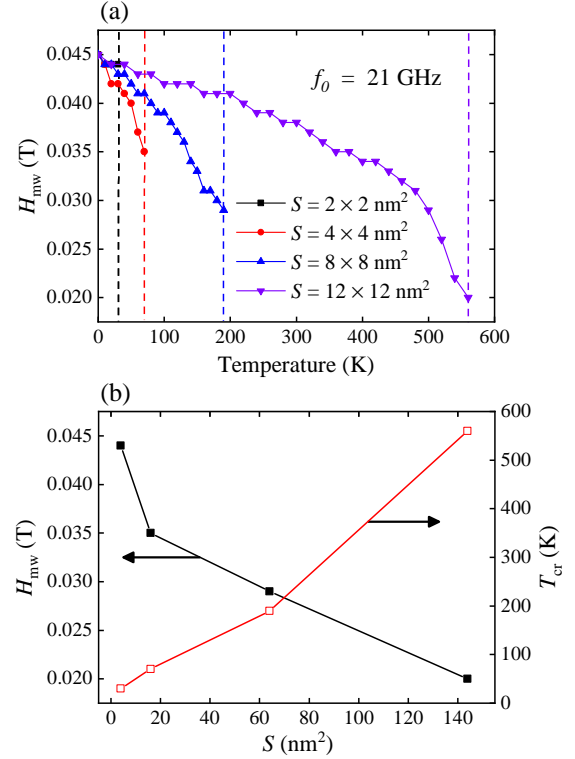


**Figure 5:** Temperature  $T$  dependence of (a)  $H_{mw}$  (while  $f_0$  and optimal  $\eta$  are constant) (b)  $H_{mw}$  (solid squares) (while  $f_0$  and optimal  $\eta$  are constant) and critical temperature  $T_{cr}$  (open squares) as a function of cross-sectional area  $S$ .

Furthermore, we investigate the thermal effect on  $H_{mw}$ , it is found that the  $H_{mw}$  decreases with temperature and for different cross-sectional area the decreasing trend is shown in the Fig. 5 (a). The vertical dashed lines indicate the critical temperature. For smaller  $S$ , the decreasing rate is faster but for the larger  $S$ , the decreasing rate is smaller. This decrements is due to the fact that the effective anisotropy and saturation magnetization decrease with temperature. Fig. 5 (b) shows the variation of the minimum required field  $H_{mw}$  and critical temperature  $T_{cr}$  as a function of  $S$ . The minimal required  $H_{mw}$  significantly decreases to  $H_{mw} = 0.035 \text{ T}$  for the  $S = 12 \times 12 \text{ nm}^2$ . The estimated critical temperature increases with  $S$  and found the  $T_{cr} \sim 360 \text{ K}$ . Therefore, it is expected that the  $H_{mw}$  ( $T_{cr}$ ) could be decreased (increased) further with enlarging the nano-particle size.

## 4. Discussion and Conclusions

With zero temperature [42], subnanosecond magnetization reversal can be achieved by the circularly polarized down-chirp microwave pulse with the critical parametric values  $H_{\text{mw}} \sim 0.045$  T,  $f_0 \sim 21$  GHz and  $\eta \sim 67.2$  ns<sup>-2</sup>. In practice, the main challenge was to generate such circularly polarized DCMWP with the parametric values mentioned above. However, when the thermal effect is included to the system, surprisingly, we observed that the amplitude  $H_{\text{mw}}$ , initial frequency  $f_0$  and chirp rate  $\eta$  of DCMWP show the decreasing trend with the increase of temperature as well as the cross-sectional area  $S$  of the system. The critical temperature also increases with the increase of  $S$ . For a system size of  $(12 \times 12)$  nm<sup>2</sup> with the temperature range 300 K to 360 K, the required values of DCMWP's parameters are estimated around  $H_{\text{mw}} \sim 0.035$  T,  $f_0 \sim 19$  GHz and  $\eta \sim 25$  to 38 ns<sup>-2</sup> which are significantly lower than that of zero temperature limit. It is expected that the required parametric values of DCMWP could be decreased further to the practically realizable limit for the larger cross-sectional area of single domain nano-particle since the macrospin model is valid up to the nano-particle diameter of 30 nm [46]. However, there are the recent technologies: the coupling a magnetic nanoparticle to a pair of weak superconducting links or by spin torque oscillator [51, 52] to generate microwave chirp pulse. Therefore, it might be feasible to generate such circularly polarized down chirp microwave pulse.

In summary, the finite thermal effect assists to achieve the fast and energy efficient magnetization reversal induced by the the DCMWP since it significantly reduces amplitude, chirp rates, and initial frequency of the DCMWP. In addition, the critical temperature increases with enlarging the system size and hence a wide operating temperature around the room temperature is possible in practice. This is happened because the energy barrier/thermal stability increases proportionately with the volume/cross-sectional area of the system, but the effective magnetization decreases with temperature, which induces faster magnetization reversal with lower energy consumption. Therefore, these findings may provide a way to realize low-cost and fast magnetization reversal with a wide operating temperature.

## 5. Acknowledgements

This work was supported by the Khulna University Research Cell (Grant No. KU/RC-04/2000-232) as well as M. A. J. P. acknowledges Ministry of Education (BANBEIS, Grant No. SD201997).

## References

- [1] S. Sun, C. B. Murray, D. Weller, L. Folks, and A. Moser, "Monodisperse fept nanoparticles and ferromagnetic fept nanocrystal superlattices," *science*, vol. 287, no. 5460, pp. 1989–1992, 2000.
- [2] S. Woods, J. Kirtley, S. Sun, and R. Koch, "Direct investigation of superparamagnetism in co nanoparticle films," *Physical review letters*, vol. 87, no. 13, p. 137205, 2001.
- [3] D. Zitoun, M. Respaud, M.-C. Fromen, M. J. Casanove, P. Lecante, C. Amiens, and B. Chaudret, "Magnetic enhancement in nanoscale corh particles," *Physical review letters*, vol. 89, no. 3, p. 037203, 2002.
- [4] B. Hillebrands and K. Ounadjela, *Spin dynamics in confined magnetic structures I & II*. Springer Science & Business Media, 2003, vol. 83.
- [5] S. Mangin, D. Ravelosona, J. Katine, M. Carey, B. Terris, and E. E. Fullerton, "Current-induced magnetization reversal in nanopillars with perpendicular anisotropy," *Nature materials*, vol. 5, no. 3, pp. 210–215, 2006.
- [6] A. Hubert, "R. schaffer, magnetic domains: the analysis of magnetic microstructures," 1998.
- [7] Z. Sun and X. Wang, "Fast magnetization switching of stoner particles: A nonlinear dynamics picture," *Physical Review B*, vol. 71, no. 17, p. 174430, 2005.
- [8] J. C. Slonczewski *et al.*, "Current-driven excitation of magnetic multilayers," *Journal of Magnetism and Magnetic Materials*, vol. 159, no. 1, p. L1, 1996.
- [9] L. Berger, "Emission of spin waves by a magnetic multilayer traversed by a current," *Physical Review B*, vol. 54, no. 13, p. 9353, 1996.
- [10] M. Tsoi, A. Jansen, J. Bass, W.-C. Chiang, M. Seck, V. Tsoi, and P. Wyder, "Excitation of a magnetic multilayer by an electric current," *Physical Review Letters*, vol. 80, no. 19, p. 4281, 1998.
- [11] J. A. Katine, F. J. Albert, R. A. Buhrman, E. B. Myers, and D. C. Ralph, "Current-driven magnetization reversal and spin-wave excitations in co/cu/cu pillars," *Phys. Rev. Lett.*, vol. 84, pp. 3149–3152, Apr 2000.
- [12] X. Waintal, E. B. Myers, P. W. Brouwer, and D. C. Ralph, "Role of spin-dependent interface scattering in generating current-induced torques in magnetic multilayers," *Phys. Rev. B*, vol. 62, pp. 12317–12327, Nov 2000.
- [13] J. Z. Sun, "Spin-current interaction with a monodomain magnetic body: A model study," *Physical Review B*, vol. 62, no. 1, p. 570, 2000.
- [14] J. Sun, "Spintronics gets a magnetic flute," *Nature*, vol. 425, no. 6956, pp. 359–360, 2003.
- [15] M. D. Stiles and A. Zangwill, "Anatomy of spin-transfer torque," *Physical Review B*, vol. 66, no. 1, p. 014407, 2002.
- [16] Y. B. Bazaliy, B. Jones, and S.-C. Zhang, "Current-induced magnetization switching in small domains of different anisotropies," *Physical Review B*, vol. 69, no. 9, p. 094421, 2004.
- [17] R. Koch, J. Katine, and J. Sun, "Time-resolved reversal of spin-transfer switching in a nanomagnet," *Physical review letters*, vol. 92, no. 8, p. 088302, 2004.
- [18] W. Wetzels, G. E. Bauer, and O. N. Jouravlev, "Efficient magnetization reversal with noisy currents," *Physical review letters*, vol. 96, no. 12, p. 127203, 2006.
- [19] A. Manchon and S. Zhang, "Theory of nonequilibrium intrinsic spin torque in a single nanomagnet," *Physical Review B*, vol. 78, no. 21, p. 212405, 2008.
- [20] I. M. Miron, G. Gaudin, S. Auffret, B. Rodmacq, A. Schuhl, S. Pizzini, J. Vogel, and P. Gambardella, "Current-driven spin torque induced by the rashba effect in a ferromagnetic metal layer," *Nature materials*, vol. 9, no. 3, pp. 230–234, 2010.
- [21] I. M. Miron, K. Garello, G. Gaudin, P.-J. Zermatten, M. V. Costache, S. Auffret, S. Bandiera, B. Rodmacq, A. Schuhl, and P. Gambardella, "Perpendicular switching of a single ferromagnetic layer induced by in-plane current injection," *Nature*, vol. 476, no. 7359, pp. 189–193, 2011.
- [22] L. Liu, C.-F. Pai, Y. Li, H. Tseng, D. Ralph, and R. Buhrman, "Spin-torque switching with the giant spin hall effect of tantalum," *Science*, vol. 336, no. 6081, pp. 555–558, 2012.
- [23] J. Grollier, V. Cros, H. Jaffres, A. Hamzic, J.-M. George, G. Faini, J. B. Youssef, H. Le Gall, and A. Fert, "Field dependence of magnetization reversal by spin transfer," *Physical Review B*, vol. 67, no. 17, p. 174402, 2003.
- [24] H. Morise and S. Nakamura, "Stable magnetization states under a spin-polarized current and a magnetic field," *Physical Review B*, vol. 71, no. 1, p. 014439, 2005.
- [25] T. Taniguchi and H. Imamura, "Critical current of spin-transfer-torque-driven magnetization dynamics in magnetic multilayers,"

- Physical Review B*, vol. 78, no. 22, p. 224421, 2008.
- [26] Y. Suzuki, A. A. Tulapurkar, and C. Chappert, "Spin-injection phenomena and applications," in *Nanomagnetism and Spintronics*. Elsevier, 2009, pp. 93–153.
- [27] Z. Sun and X. Wang, "Theoretical limit of the minimal magnetization switching field and the optimal field pulse for stoner particles," *Physical review letters*, vol. 97, no. 7, p. 077205, 2006.
- [28] X. Wang and Z. Sun, "Theoretical limit in the magnetization reversal of stoner particles," *Physical review letters*, vol. 98, no. 7, p. 077201, 2007.
- [29] X. Wang, P. Yan, J. Lu, and C. He, "Euler equation of the optimal trajectory for the fastest magnetization reversal of nano-magnetic structures," *EPL (Europhysics Letters)*, vol. 84, no. 2, p. 27008, 2008.
- [30] G. Bertotti, C. Serpico, and I. D. Mayergoyz, "Nonlinear magnetization dynamics under circularly polarized field," *Physical Review Letters*, vol. 86, no. 4, p. 724, 2001.
- [31] Z. Sun and X. Wang, "Strategy to reduce minimal magnetization switching field for stoner particles," *Physical Review B*, vol. 73, no. 9, p. 092416, 2006.
- [32] J.-G. Zhu and Y. Wang, "Microwave assisted magnetic recording utilizing perpendicular spin torque oscillator with switchable perpendicular electrodes," *IEEE Transactions on Magnetics*, vol. 46, no. 3, pp. 751–757, 2010.
- [33] C. Thirion, W. Wernsdorfer, and D. Maily, "Switching of magnetization by nonlinear resonance studied in single nanoparticles," *Nature materials*, vol. 2, no. 8, pp. 524–527, 2003.
- [34] K. Rivkin and J. B. Ketterson, "Magnetization reversal in the anisotropy-dominated regime using time-dependent magnetic fields," *Applied physics letters*, vol. 89, no. 25, p. 252507, 2006.
- [35] Z. Wang and M. Wu, "Chirped-microwave assisted magnetization reversal," *Journal of Applied Physics*, vol. 105, no. 9, p. 093903, 2009.
- [36] N. Barros, M. Rassam, H. Jirari, and H. Kachkachi, "Optimal switching of a nanomagnet assisted by microwaves," *Physical Review B*, vol. 83, no. 14, p. 144418, 2011.
- [37] N. Barros, H. Rassam, and H. Kachkachi, "Microwave-assisted switching of a nanomagnet: Analytical determination of the optimal microwave field," *Physical Review B*, vol. 88, no. 1, p. 014421, 2013.
- [38] G. Klughertz, P.-A. Hervieux, and G. Manfredi, "Autoresonant control of the magnetization switching in single-domain nanoparticles," *Journal of Physics D: Applied Physics*, vol. 47, no. 34, p. 345004, 2014.
- [39] S. I. Denisov, T. V. Lyutyy, P. Hänggi, and K. N. Trohidou, "Dynamical and thermal effects in nanoparticle systems driven by a rotating magnetic field," *Physical Review B*, vol. 74, no. 10, p. 104406, 2006.
- [40] S. Okamoto, N. Kikuchi, and O. Kitakami, "Magnetization switching behavior with microwave assistance," *Applied Physics Letters*, vol. 93, no. 10, p. 102506, 2008.
- [41] T. Tanaka, Y. Otsuka, Y. Furomoto, K. Matsuyama, and Y. Nozaki, "Selective magnetization switching with microwave assistance for three-dimensional magnetic recording," *Journal of Applied Physics*, vol. 113, no. 14, p. 143908, 2013.
- [42] M. T. Islam, X. Wang, Y. Zhang, and X. Wang, "Subnanosecond magnetization reversal of a magnetic nanoparticle driven by a chirp microwave field pulse," *Physical Review B*, vol. 97, no. 22, p. 224412, 2018.
- [43] R. H. Koch, G. Grinstein, G. Keefe, Y. Lu, P. Trouilloud, W. Gallagher, and S. Parkin, "Thermally assisted magnetization reversal in submicron-sized magnetic thin films," *Physical review letters*, vol. 84, no. 23, p. 5419, 2000.
- [44] Z. Li and S. Zhang, "Thermally assisted magnetization reversal in the presence of a spin-transfer torque," *Physical Review B*, vol. 69, no. 13, p. 134416, 2004.
- [45] J. De Vries, T. Bolhuis, and L. Abelmann, "Temperature dependence of the energy barrier and switching field of sub-micron magnetic islands with perpendicular anisotropy," *New journal of physics*, vol. 19, no. 9, p. 093019, 2017.
- [46] J. M. Iwata-Harms, G. Jan, H. Liu, S. Serrano-Guisan, J. Zhu, L. Thomas, R.-Y. Tong, V. Sundar, and P.-K. Wang, "High-temperature thermal stability driven by magnetization dilution in cofeb free layers for spin-transfer-torque magnetic random access memory," *Scientific reports*, vol. 8, no. 1, pp. 1–7, 2018.
- [47] W. Liu, B. Cheng, S. Ren, W. Huang, J. Xie, G. Zhou, H. Qin, and J. Hu, "Thermally assisted magnetization control and switching of dy3fe5o12 and tb3fe5o12 ferrimagnetic garnet by low density current," *Journal of Magnetism and Magnetic Materials*, p. 166804, 2020.
- [48] T. L. Gilbert, "A phenomenological theory of damping in ferromagnetic materials," *IEEE transactions on magnetics*, vol. 40, no. 6, pp. 3443–3449, 2004.
- [49] A. Vansteenkiste, J. Leliaert, M. Dvornik, M. Helsen, F. Garcia-Sanchez, and B. Van Waeyenberge, "The design and verification of mumax3," *AIP advances*, vol. 4, no. 10, p. 107133, 2014.
- [50] M. T. Islam, X. Wang, and X. Wang, "Thermal gradient driven domain wall dynamics," *Journal of Physics: Condensed Matter*, vol. 31, no. 45, p. 455701, 2019.
- [51] L. Cai, D. A. Garanin, and E. M. Chudnovsky, "Reversal of magnetization of a single-domain magnetic particle by the ac field of time-dependent frequency," *Physical Review B*, vol. 87, no. 2, p. 024418, 2013.
- [52] L. Cai and E. M. Chudnovsky, "Interaction of a nanomagnet with a weak superconducting link," *Physical Review B*, vol. 82, no. 10, p. 104429, 2010.